

# AUTONOMOUS ORBIT CONTROL PROCEDURE, USING A SIMPLIFIED GPS NAVIGATOR, APPLIED TO THE CBERS SATELLITE

**Roberto Luiz Galski\***  
**Valcir Orlando**  
**Hélio Koiti Kuga**

*INPE – Instituto Nacional de Pesquisas Espaciais  
CP 515 – São José dos Campos, SP  
CEP 12201-970 Brazil  
\*E-Mail: galski@ccs.inpe.br*

**ABSTRACT** – *This work<sup>1</sup> presents the performance analysis of a proposed autonomous orbit control procedure, when applied to a simulation of CBERS-1, the first China-Brazil Earth Resources Satellite. A simplified GPS navigator is used in the feedback control loop, in order to supply the needed autonomous orbit information. The simplified navigator consists of a Kalman filtering process, which incorporates a procedure for automatic treatment of observation biases. The results on a long-term computer simulation (one year), which indicate the feasibility of the proposed autonomous orbit control procedure, are presented, discussed, and compared with related previous works.*

**KEYWORDS:** Autonomous Orbit Control, GPS, Autonomous Navigator, Kalman Filter.

## INTRODUCTION

This work presents the performance analysis of a proposed autonomous orbit control procedure when applied in a simulation to the China-Brazil Earth Resources Satellite – CBERS [1] (successfully launched on October 14, 1999). There, a simplified GPS navigator is used in the feedback control loop, in order to supply the needed autonomous orbit observations. The idea behind using a simplified navigator is to allow the computation of improved orbit estimates from the GPS (geometric) navigation solution [2], without adding a significant computational burden to the autonomous orbit control procedure. Typical root mean square errors of the coarse GPS geometric estimates were of 100m in position and 1m/s in velocity, before Selective Availability was turned off. Added to such random errors these estimates showed systematic variations with values of the order of 100m and duration of about 1 to 15 minutes [3]. The simplified navigator consists, basically, of a Kalman filtering process, which incorporates a procedure for automatic treatment of observation biases. On the other hand, the goal of the control is to provide autonomous control of the Equator longitude phase drift ( $\Delta L_0$ ) of low-Earth phased orbits, thanks to the on-board availability of orbit estimates, autonomously generated by the navigator. In a previous work the performance of an autonomous orbit control procedure was analyzed considering the direct use, in the feedback loop, of the coarse GPS navigation solution[4]. That work considered a hypothetical

---

<sup>1</sup> This work has been supported by CNPq (Comissão Nacional de Desenvolvimento Científico e Tecnológico)

satellite, equipped with a GPS navigator receiver, placed in a phased helio-synchronous orbit. Under worse case conditions in terms of solar activity, considered in a previous investigation, the autonomous control successfully maintained the drift  $\Delta L_0$  restricted to an excursion range of about -1000m and 1700m. The specified nominal  $\Delta L_0$  range for the CBERS-1 is  $\pm 10,000$ m. The current work, by introducing the simplified navigator to the autonomous control procedure, successfully improved the control results, significantly reducing the variation range of  $\Delta L_0$ . Both realistic and worse case conditions in terms of solar activity were considered in the simulation. The study has been carried out considering the application of a version of the autonomous orbit control procedure [5], which considers only the application of semi-major axis corrections with a constant, previously chosen amplitude. Some improvements have, however, been implemented. In the original version the raw observation of both  $\Delta L_0$  and its first time derivative,  $\dot{\Delta L}_0$ , were computed from each simulated set of GPS orbit estimates. Now only the  $\Delta L_0$  observations are computed from the orbit estimates. The needed observations of  $\dot{\Delta L}_0$  are directly computed, in a numerical way, from the last computed observations of  $\Delta L_0$ . Such approach increased the accuracy of the  $\dot{\Delta L}_0$  observations and, as a consequence, the performance of the autonomous control process. A maximal maneuver application rate of about one pulse per orbit was considered. It was also considered a GPS observation rate (and consequently the navigator output rate) of 1 estimate each 9 seconds. Only one among 20 orbit estimates sets successively issued by the navigator is used by the control system. The results which indicate the feasibility of the application of the simplified GPS navigator to the autonomous orbit control system on a long-term computer simulation (one year), are presented, discussed, and compared with the previously mentioned investigation.

## SIMPLIFIED GPS NAVIGATOR

The aim of the simplified navigator is to improve the accuracy of the GPS coarse navigation solution, by processing its position coordinates by a Kalman filtering procedure with an automatic treatment of observation biases. The basic idea is to model the bias in these coordinates as a stochastic process, and add the so modeled bias to the orbit dynamic equations. The Extended Kalman Filter is then applied to this increased dimension system, in order to estimate the observation bias components together with the orbit state vector. The main feature of this Kalman filtering process is to automatically compensate for the effect of observation bias on the position and velocity components of the satellite orbit.

In the propagation phase of the Kalman filter it is used a simplified orbit model that just includes the development of force due to the geopotential, considering spherical harmonics only until the zonal coefficient  $J_2$ . In vector form the considered orbit dynamic model, in Cartesian coordinates, is:

$$\dot{\mathbf{x}}(t) = \mathbf{f}[\mathbf{x}(t), t] + \mathbf{G}(t) \boldsymbol{\omega}(t) \quad (1)$$

where:  $\mathbf{x}(t) = [x1(t) \ x2(t) \ x3(t) \ x4(t) \ x5(t) \ x6(t)]^T$  is the orbit state vector; composed by the position ( $x1, x2, x3$ ) and velocity ( $x4, x5, x6$ ) components;  $[ \cdot ]^T$  means the transpose of the related vector or matrix;  $\mathbf{f}[\mathbf{x}(t), t]$  is a 6<sup>th</sup> dimension vector of non-linear functions of the orbital state;  $\mathbf{G}(t)$  is a continuous 6x3 matrix;  $\boldsymbol{\omega}(t)$  is a 3<sup>rd</sup> dimension vector which represents the uncertainties in the knowledge of the forces acting on the satellite. The vector  $\boldsymbol{\omega}(t)$  is assumed to be composed of gaussian white noise, with zero mean and matrix of spectral power density  $\mathbf{Q}(t)$ . The matrix,  $\mathbf{G}(t)$  matrix is of the form:

$$\mathbf{G} = [0_{3 \times 3} \ I_{3 \times 3}]^T \quad (2)$$

Only the position coordinates of the coarse solution supplied by GPS receivers will be used as observations for the Kalman filtering process, disregarding the less accurate velocity coordinates. The observation vector in the instant  $t_{k+1}$  is modeled as:

$$\mathbf{y}(t_{k+1}) = \mathbf{H} \mathbf{x}(t_{k+1}) + \mathbf{e}(t_{k+1}) + \mathbf{v}(t_{k+1}) \quad (3)$$

where  $\mathbf{H} = [ \mathbf{I}_{3 \times 3} \quad \mathbf{0}_{3 \times 3} ]$ ,  $\mathbf{e}(t_{k+1})$  is a 3<sup>rd</sup> dimension vector of the observation bias;  $\mathbf{v}(t_{k+1})$  is 3<sup>rd</sup> dimension vector of random errors, assumed to be gaussian white noise with zero mean and covariance matrix given by the 3x3 matrix  $\mathbf{R}(t_{k+1})$ .

The bias of the GPS observations (on position components of the GPS coarse navigation solution), as commented previously, change their values whenever changes the set of GPS satellites which are used by the GPS receiver. They stay constant for periods between 1 to 15 minutes. Whenever a GPS satellite leaves or enters the receiver visibility region, a change in the bias values occurs. To take into account these observation bias variations, the following modeling is considered for the bias vector:

$$\dot{\mathbf{e}}(t) = \boldsymbol{\omega}_e(t) \quad (4)$$

where  $\boldsymbol{\omega}_e(t)$  is a 3<sup>rd</sup> dimension vector, which represents the uncertainty in the adopted observation bias model (assumed as constants, according to Equation 4). It is supposed that  $\boldsymbol{\omega}_e(t)$  follows a Gaussian distribution with zero mean and covariance matrix given by the 3x3 matrix  $\mathbf{Q}_e$ . The initial value  $\mathbf{e}(t_0)$  is considered as a vector of gaussian random variables, with mean  $\hat{\mathbf{e}}(t_0)$  and covariance matrix  $\mathbf{P}_e(t_0)$ , where  $\hat{\mathbf{e}}(t_0)$  and  $\mathbf{P}_e(t_0)$  are a priori estimates. It is assumed that  $\mathbf{v}(t_k)$  is non-correlated with  $\boldsymbol{\omega}_e(t)$  and  $\hat{\mathbf{e}}(t_0)$ .

Now, defining the following augmented system state vector:

$$\mathbf{x}_A(t) \equiv [\mathbf{x}(t) \quad \mathbf{e}(t)]^T, \quad (5)$$

and having in mind Equation 1, one can write:

$$\dot{\mathbf{x}}_A(t) = \mathbf{f}_A[\mathbf{x}_A(t), t] + \mathbf{G}_A(t) \boldsymbol{\omega}(t), \quad (6)$$

where:  $\mathbf{f}_A[\mathbf{x}_A(t), t] \equiv [\mathbf{f}_A[\mathbf{x}_A(t), t] \quad \mathbf{0}_{3 \times 1}]^T$ ;  $\boldsymbol{\omega}_A(t) \equiv [\boldsymbol{\omega}(t) \quad \boldsymbol{\omega}_e(t)]^T$ ; and  $\mathbf{G}_A \equiv \begin{bmatrix} \mathbf{G} & \mathbf{0}_{6 \times 3} \\ \mathbf{0}_{3 \times 3} & \mathbf{I}_{3 \times 3} \end{bmatrix}$ .

Considering the definition of  $\mathbf{x}_A(t)$ , given by Equation 5 then, the observation equation (Equation 3) can be put in the form:

$$\mathbf{y}(k+1) = \mathbf{H}_A \mathbf{x}_A(t_{k+1}) + \mathbf{v}(t_{k+1}) \quad (7)$$

where:  $\mathbf{H}_A = [ \mathbf{I}_{3 \times 3} \quad \mathbf{0}_{3 \times 3} \quad \mathbf{I}_{3 \times 3} ]$ . Considering the above definitions the error covariance matrix of the augmented state estimates and of dynamic system modeling takes the form:

$$\mathbf{Q}_A = \begin{bmatrix} \mathbf{Q}_{3 \times 3} & \mathbf{0}_{3 \times 3} \\ \mathbf{0}_{3 \times 3} & \mathbf{Q}_e_{3 \times 3} \end{bmatrix}; \quad \mathbf{P}_A = \begin{bmatrix} \mathbf{P}_{6 \times 6} & \mathbf{0}_{6 \times 3} \\ \mathbf{0}_{3 \times 6} & \mathbf{P}_e_{3 \times 3} \end{bmatrix}. \quad (8)$$

Applying the extended Kalman filter to the augmented system just defined, and accounting for the adopted assumptions, one has:

- **Time Update Phase:**

$$\hat{\mathbf{x}}_A(t_{k+1}/t_k) = \hat{\mathbf{x}}_A(t_k/t_k) + \int_{t_k}^{t_{k+1}} \mathbf{f}_A[\mathbf{x}_A(t), t] dt \quad (9)$$

$$\mathbf{P}_A(t_{k+1}/t_k) = \boldsymbol{\phi}_A[t_{k+1}/t_k; \hat{\mathbf{x}}_A(t_k/t_k)] \cdot \mathbf{P}_A(t_k/t_k) \cdot \boldsymbol{\phi}_A^T[t_{k+1}/t_k; \hat{\mathbf{x}}_A(t_k/t_k)] + \boldsymbol{\Gamma}_A(t_k) \cdot \mathbf{Q}_A(t_k) \cdot \boldsymbol{\Gamma}_A^T(t_k) \quad (10)$$

where:

$$\boldsymbol{\Gamma}_A(t_k) = \int_{t_k}^{t_{k+1}} \boldsymbol{\phi}_A[t_{k+1}, \tau] \mathbf{G}_A(\tau) d\tau, \quad \text{and} \quad \boldsymbol{\phi}_A[t_{k+1}/t_k; \hat{\mathbf{x}}_A(t_k/t_k)] = \begin{bmatrix} \boldsymbol{\phi}_{6 \times 6} & \mathbf{0}_{6 \times 3} \\ \mathbf{0}_{3 \times 6} & \mathbf{I}_{3 \times 3} \end{bmatrix} \quad (11)$$

- **Measurement Update Phase:**

$$\hat{\mathbf{x}}_A(t_{k+1}/t_{k+1}) = \hat{\mathbf{x}}_A(t_{k+1}/t_k) + \mathbf{K}[t_{k+1}; \hat{\mathbf{x}}_A(t_{k+1}/t_k)] \cdot \{ \mathbf{y}(t_{k+1}) - \mathbf{H}_A \hat{\mathbf{x}}_A(t_{k+1}/t_k) \} \quad (12)$$

$$\mathbf{P}_A(t_{k+1}/t_{k+1}) = \{ \mathbf{I} - \mathbf{K}[t_{k+1}; \hat{\mathbf{x}}_A(t_{k+1}/t_k)] \cdot \mathbf{H}_A \} \cdot \mathbf{P}_A(t_{k+1}/t_k) \quad (13)$$

where

$$\mathbf{K}[t_{k+1}; \hat{\mathbf{x}}_A(t_{k+1}/t_k)] = \mathbf{P}_A(t_{k+1}/t_k) \cdot \mathbf{H}_A^T \cdot \{ \mathbf{H}_A \cdot \mathbf{P}_A(t_{k+1}/t_k) \cdot \mathbf{H}_A^T + \mathbf{R}(t_{k+1}) \}^{-1} \quad (14)$$

Since the observation biases are estimated together with the satellite orbit state, their effects on the orbit estimates are automatically compensated for, improving, in this way, the accuracy of these estimates.

### Simulation of the GPS Coarse Navigation Solution

Each GPS satellite transmits two signs for the positioning, modulated with two code types: P and C/A. The C/A code (Coarse/Acquisition) it is of civil use and it is always transmitted, being subject to degradations. The code P (precise) is reserved for military use and authorized users. The precision of the C/A sign could be degraded by the application of intentional degradation of GPS satellites clock information, or by incorporating small errors in the transmitted ephemeris. This kind of degradation, named Selective Readiness (or Selective Availability - SA) has been disabled by the Department of Defense of USA in 2000. In spite of this, in this work, one will simulate the GPS coarse navigation solution considering the Selective Availability activated, in order to deal with worst case conditions. Thus, the random errors in the position and velocity components of the GPS coarse navigation solution were simulated with 100m and 1m/s standard deviations [6], respectively. Added to such random errors these estimates show systematic variations with values of the order of 100m (position) and 0.5m/s (velocity), and duration of about 1 to 15 minutes. This was simulated by considering standard deviation of 25m and 0.125m/s in each component of position and velocity vectors, respectively. As previously mentioned, these systematic variations occur due to the changes of the visible set of GPS satellites to the on-board receiver. Each GPS satellite has its own systematic error. For this reason, whenever a satellite goes into or out of the GPS receiver antenna coverage region, the systematic error of the global navigation solution is prone to change its value.

### Simplified Navigator Test Results

A performance analysis of the simplified autonomous GPS navigator was accomplished with help of a realistic simulation of the CBERS-1 orbit. It was considered in this analysis the observation rate of one set of GPS coarse orbit estimates each 9 seconds. The results will be presented and commented in what follows, in terms of the parameters  $\Delta r_{GPS}$ , error with respect to coarse GPS navigation solution;  $\Delta r_{NAV}$ , error with respect to Kalman filter estimates; and  $\Delta \hat{r}_{NAV}$  estimated error:

$$\Delta r_{GPS}(t_k) = \left\{ \sum_{i=1}^3 [x_i(t_k) - x_{GPS_i}(t_k/t_k)]^2 \right\}^{1/2} \quad (15)$$

$$\Delta r_{NAV}(t_k) = \left\{ \sum_{i=1}^3 [x_i(t_k) - \hat{x}_i(t_k/t_k)]^2 \right\}^{1/2} \quad (16)$$

$$\Delta \hat{r}_{NAV}(t_k) = \left\{ \sum_{i=1}^3 P_{Aii}(t_k/t_k) \right\}^{1/2} \quad (17)$$

where  $x_i(t_k)$ ,  $i = 1, 2, 3$  represents the first three components (position) of the reference (simulated) orbit state vector;  $x_{GPS_i}(t_k/t_k)$ ,  $i = 1, 2, 3$  represents the first three components (position) of the simulated GPS coarse navigation solution;  $\hat{x}_i(t_k/t_k)$ ,  $i = 1, 2, 3$  represents the first three components (position) of the estimated state vector; and  $P_{ii}(t_k/t_k)$ ,  $i = 1, 2, 3$  are the first three elements of the diagonal of the

covariance matrix of the orbit estimate errors. The Fig. 1 presents the values of  $\Delta r_{GPS}$ ,  $\Delta r_{NAV}$ , and  $\Delta \hat{r}_{NAV}$  obtained when the Kalman filtering process does not include the procedure for automatic treatment of the observation bias

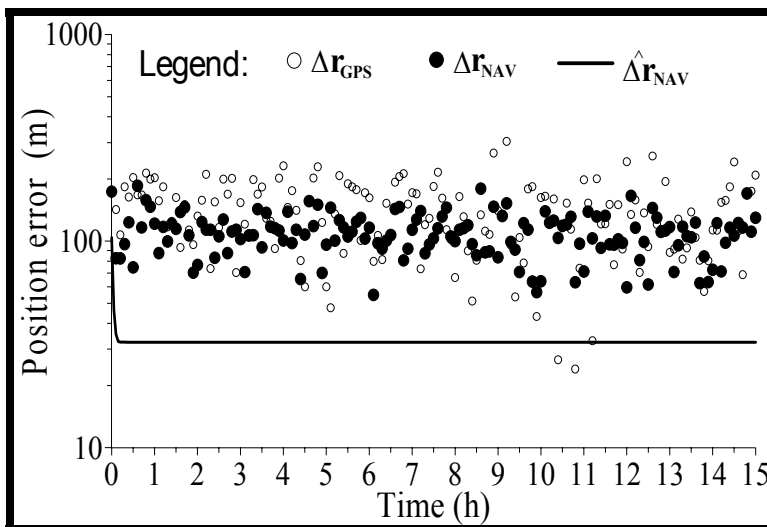


**Fig. 1. Orbit Estimation Results Without Automatic Treatment of Observation Bias**

The Fig. 1 clearly shows the divergence of the Kalman filtering process, since the magnitudes of the estimated error ( $\Delta \hat{r}_{NAV}$ ) remains smaller than the real ones ( $\Delta r_{NAV}$ ). It is also to be observed, that the real errors in the position coordinates estimates presents a greater dispersion and are of the same order of magnitude than the ones of the simulated GPS coarse navigation solution, used as observations by the filtering process. As far as the velocity components are concerned, the same kind of results was obtained. The bad performance presented by the Kalman filtering process shows the impossibility of improving the precision of the GPS coarse navigation solution, without considering the use of some kind of procedure to deal with the observation biases.

Fig. 2 presents a graphical similar to the one of Fig. 1, showing now the results obtained with the application of the proposed simplified navigator, where the procedure for automatic treatment of the observation biases are considered.

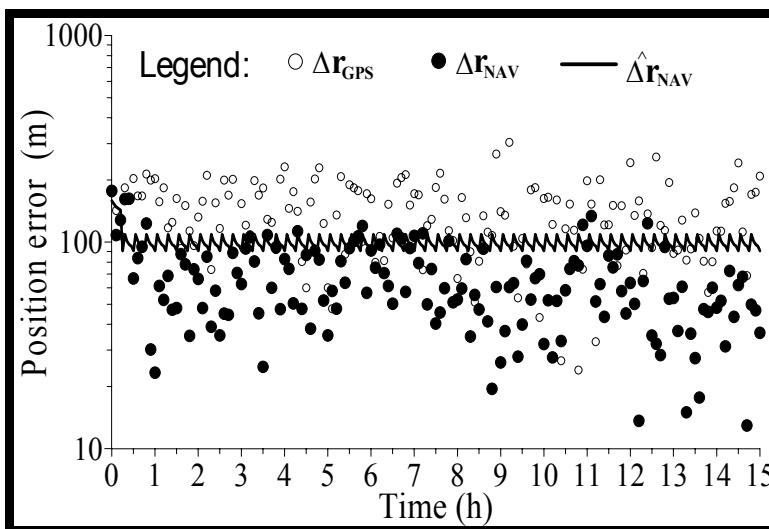


**Fig. 2. Simplified Navigator Results**

As one can see by Fig. 2, in the current case where the procedure for automatic treatment of observation biases is considered, the Kalman filtering process filter presented a satisfactory performance. The real error, as can be seen from Fig. 2, is of the order of two times lower than the one corresponding to the GPS coarse navigation solution. In view of the simplicity of the proposed navigator, this can be considered as a very promising result. The filter showed also good characteristics in terms of robustness, since it does not presented any sign of divergence during all simulated period. The peaks presented by the curve of  $\Delta \hat{r}_{NAV}$  are caused by the re-initialization of the estimation process, every time a change of the values of the observation bias occurs. The results concerning the velocity components of the orbit state vector showed very similar performance to the presented position estimates.

## AUTONOMOUS CONTROL PROCEDURE

### Procedure Description

Fig. 3 presents the block diagram of the autonomous control system, depicting how it was simulated.

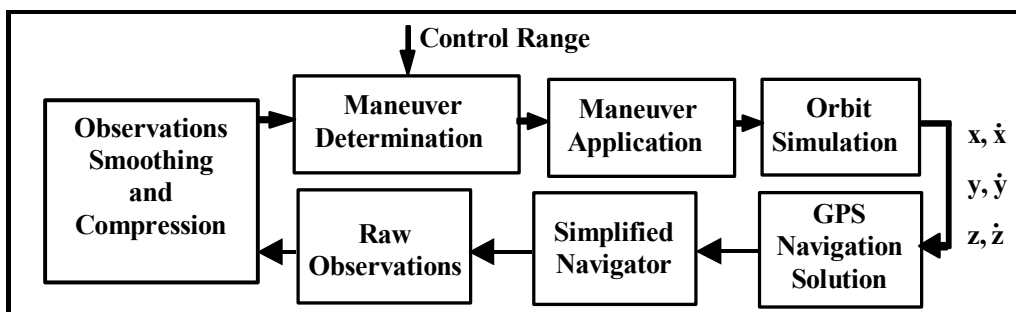


**Fig. 3. Block Diagram of the Autonomous Control System**

The GPS navigation solution estimates are computed with help of a realistic orbit simulation process. The position components of these estimates are, in what follows, taken as observations by the GPS simplified navigator. Then, from each set of improved orbit estimates issued by the simplified navigator, raw observations of  $\Delta L_0$  are computed. These raw observations are preprocessed in real time, in order to achieve data smoothing by curve fitting, validation and redundancy reduction. Observation of  $\dot{\Delta L}_0$  and  $\ddot{\Delta L}_0$  are numerically derived from the smoothed values of  $\Delta L_0$ . The computed observations (including the observations of  $\dot{\Delta L}_0$  and  $\ddot{\Delta L}_0$ ) are, finally, used within the Maneuver Determination process, where the instants of orbit correction applications are defined. One maneuver is considered needed when the following condition is verified:

$$\hat{\Delta L}_0(t_k) > \Delta L_{0sup} - n \cdot \sigma(t_k) \quad (18)$$

with,

$$\Delta L_{0sup} = \Delta L_{0supn} \cdot [k_0 - k_1 \cdot \dot{\Delta L}_0(t_k) - k_2 \cdot \ddot{\Delta L}_0(t_k)] \quad (19)$$

where:  $\Delta L_{0supn}$  is a previously chosen control limit;  $\sigma(t_k)$  is the standard deviation of  $\hat{\Delta L}_0(t_k)$  and  $n$ ,  $k_0$ ,  $k_1$  and  $k_2$  are real numbers. Closing the simulation loop, an orbit maneuver is autonomously executed whenever the Maneuver Determination process determines a need of orbit correction.

It will be shown a version of the autonomous control procedure, in which only constant semi-major axis corrections are applied to the satellite, in order to correct the time evolution of  $\Delta L_0$ . By this procedure, there is no computation of orbit correction amplitudes. The amplitudes of corrections have always the

same pre-determined value, independent of the current conditions in terms of navigation error magnitude and solar activity. Every time the conditions given by Equations 18 and 19 are both satisfied one semi-major axis increment, with the constant pre-determined amplitude, are applied to correct the time evolution of  $\Delta L_0$ .

### Autonomous Control Test Results

The performance of the improved (by the use of the simplified navigator based on GPS) autonomous orbit control procedure, was verified through the execution of a realistic simulation of its application to a CBERS-like satellite. The simulation covered a period of about one-year, under unrealistically worse case conditions in terms of solar activity variation. Realistic (moderated) and critical conditions in terms of solar activities, shown in Fig. 4, were considered in the analysis. The critical solar flux profile, the left plot of Fig. 4, compresses the 11-year cycle to one-year simulation, with a very high maximum (360 in flux units), and keeps the 27-day cycle oscillations due to solar rotation.

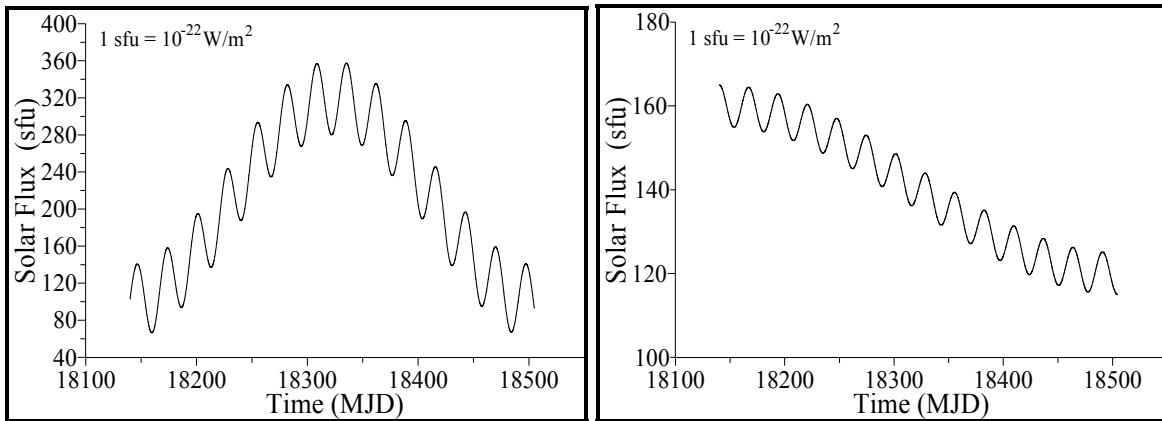


**Fig. 4. Critical and Moderate Solar Profiles Considered in the Tests**

Fig. 5 presents the curve of  $\Delta L_0$  vs. time obtained in a previous analysis [4], where a GPS like coarse navigation solution was directly used to generate the raw  $\Delta L_0$  observations. Critical solar activity profile, and maximal allowable maneuver rate of 1 orbit correction per orbit was considered.

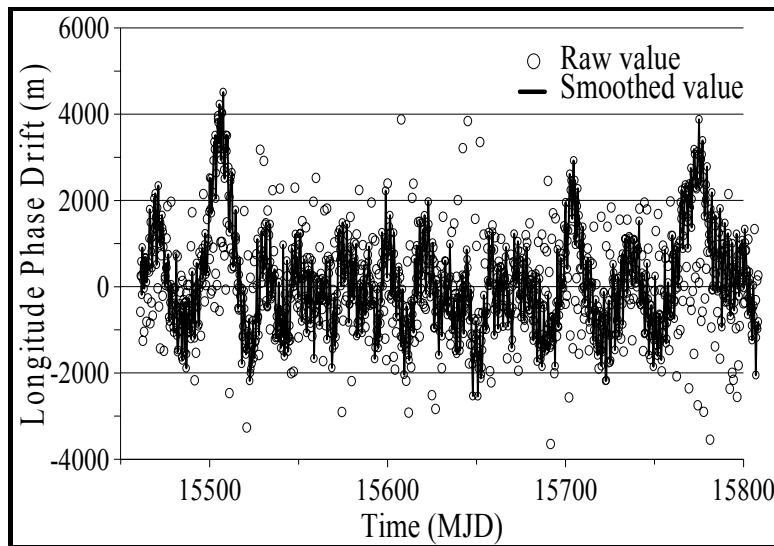


**Fig. 5. Time Evolution of  $\Delta L_0$  When the Simplified GPS Navigator is Not Used**

As one can see from Fig. 5, the values of  $\Delta L_0$  remained, during almost all the simulated period, inside the range of -2000m to +4000m. The results could, however, be considered satisfactory, since the values of  $\Delta L_0$  remained inside a range, which is, in the worst case, less than half of the allowable  $\Delta L_0$  range specified for the CBERS-1 orbit control.

The results of the current work, considering the incorporation of the GPS simplified navigator to the autonomous control system, under critical solar activity condition, are shown in Fig. 6. The same observation rate above considered for the simplified navigator analysis was considered. Although the navigator supplies orbit estimates at a rate of 1 set each 9 seconds, the autonomous control procedure only used one of such sets each 9 minutes. This could be done because it was realized that the navigator presented a good performance operating at such high observation rate, for the autonomous control; however, this rate presented a too high redundancy of information about  $\Delta L_0$ . As previously commented, an additional data smoothing and compression procedure is applied inside the controller, in order to improve the estimation of the mean evolution of  $\Delta L_0$ . The autonomous orbit control procedure was implemented in such a way that the chosen compression rate determines the maximal allowable maneuver application rate. In the current analysis it was considered the compression rate (and, as a consequence, the maximal allowable maneuver rate) of 1 each 100 minutes (about one orbit period), and the amplitude of 3m for every semi-major axis correction.

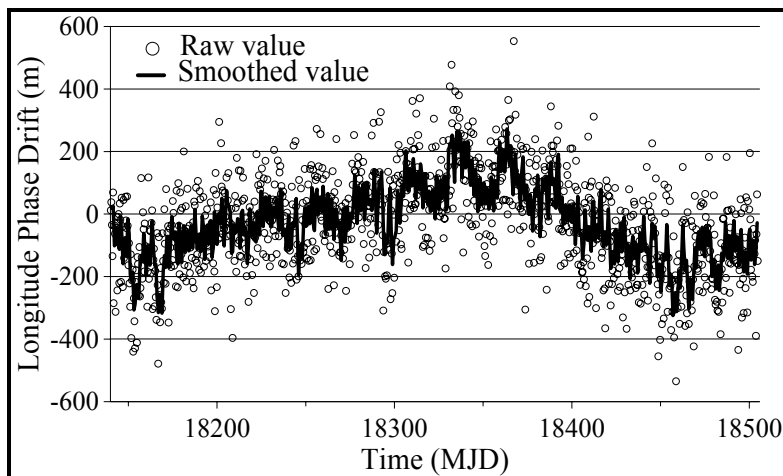


**Fig. 6.  $\Delta L_0$  vs. Time: Use of Simplified GPS Navigator, Under Critical Solar Activity**

By comparing the results of the current investigation, depicted in Fig. 6, with the ones related to a previous analysis, presented in Fig. 5, one can see that the inclusion of the simplified navigator to the autonomous orbit control procedure produced a significant reduction in the variation range of  $\Delta L_0$ . The mean (smoothed) value of  $\Delta L_0$  remained in a range of about  $\pm 300$ m, which is about one order of magnitude lower than the previous case shown in Fig. 5, where the coarse navigation solution was directly used in the autonomous control procedure. By improving the accuracy of the GPS coarse navigation solution, the use of the simplified navigator allowed, as expected, to obtain a consequent improvement of the autonomous control performance. The obtained results can be considered very promising. They reveal that a very relevant increment in the autonomous control accuracy can be obtained, with a relatively low increment in terms of the overall computational load imposed to the controller by the simplified navigator. In addition, these results indirectly show satisfactory robustness characteristics of the simplified GPS navigator, since the accomplished tests considered, always, a long simulated period (about one year). It can be inferred from Fig. 6 that, during the entire simulated period, the navigator performed very conveniently, since any degradation occurred in the navigator performance would have no impact in the overall performance of the autonomous control system.

Fig. 7 presents the results obtained when moderate conditions in terms of solar activity were considered. All the other conditions cited in the case of the Fig. 6 were also been considered in the current one.

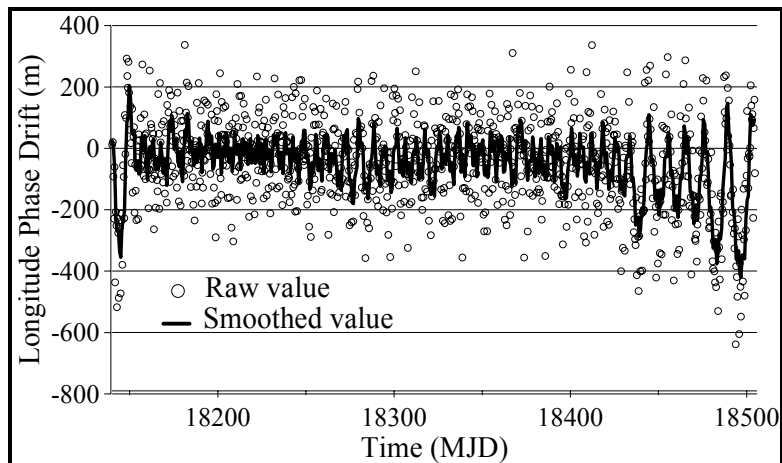


**Fig. 7.  $\Delta L_0$  vs. Time: Use of Simplified GPS Navigator, Under Moderate Solar Activity**

We observe from Fig. 7 that the values of  $\Delta L_0$  remained in a variation range a little smaller than the one obtained under critical solar activity conditions (Fig. 6). The plot presents a behavior a little more stable than the one of Fig. 6. The increasing trend presented by the curve of Fig. 6, in the central region of the graphics, where the values of the critical solar flux conditions (Fig. 4) are higher, did not occur, as it could be expected, in the case of moderated solar activity condition.

## CONCLUSIONS

The simplified GPS navigator with automatic compensation of observation biases, presented very satisfactory results in the performed simulation tests. It attained the prescribed objective of significantly improving the orbit estimates corresponding to the coarse GPS navigation solution. It was shown the feasibility of reducing the existing systematic error in the position and velocity components of the GPS coarse solution by a factor of, respectively, the order of 60% and 85%. In addition, the developed autonomous navigator showed to have good robustness characteristic. In all performed long term simulations the Kalman filtering process did not present any divergence problem. It can, in this way, be concluded that the estimator re-initialization process (which is applied after each abrupt variation of the observation biases, that happens after each change of the set of visible GPS satellites) was very efficient in the task of avoiding filter divergence.

The inclusion of the simplified navigator to the autonomous orbit control procedure also was shown to be very promising. Concerning this subject, one can say that the results were quite satisfactory. As expected, the use of more accurate orbit estimates in the computation of the needed observations of the phase drift  $\Delta L_0$  improved the performance of the autonomous orbit control. Even under worse case conditions, in terms of solar activity, the longitude phase drift was maintained by the controller inside a reduced range of  $\pm 300$ m. This represents a relevant gain in terms of accuracy when compared with the results of a previous work, where the coarse GPS navigation solution was directly applied in the orbit control process. In this previous work, where critical solar flux conditions were also considered, the values of  $\Delta L_0$  remained inside a very larger range of about -1000 m to +2000m. It should also be remarked that the use of the second derivative of  $\Delta L_0$ , in order to infer the current solar activity condition for the maneuver determination process, has also contributed in to increment the autonomous control performance.

Another positive aspect which must be mentioned is that, due to the navigator simplicity, the obtained gain in terms of autonomous control performance did not imply in a prohibitive rise to the computer processing burden.

## REFERENCES

- [1] H.K. Kuga, P.R. Prasad, V. Carrara, "Flight Dynamics Analysis and Operational Support for "CBERS", *Journal of the Brazilian Society of Mechanical Sciences*, Vol. XXI - Special Issue, 1999.
- [2] E. Gill, "Orbit Determination of the MIR Space Station from GPS Navigation Data", *Proceedings of the 12<sup>th</sup> International Symposium on Space Flight Dynamics*, Darmstadt, Germany, June 1997, pp. 79-84.
- [3] R.C. Hart, S. Truong, A.C. Long,, T. Lee, J. Chan, D.H. Oza, "GPS Navigation Initiatives at Goddard Space Flight Center Flight Dynamics Division", *Advances in the Astronautical Sciences, American Astronautical Society Publication*, Vol. 95, Part 1, 1997, pp. 315-327.
- [4] V. Orlando, H.K. Kuga, "Effect Analysis of the Maximal Allowable Maneuver Application Rate for an Autonomous Orbit Control Procedure Using GPS," *International Symposium on Space Dynamics*, Biarritz, France, July, 2000.
- [5] V. Orlando, H. K. Kuga, "Analysis of an Autonomous Orbit Control Concept Using GPS", *Journal of the Brazilian Society of Mechanical Sciences*, Vol. XXI, Special Issue, February 1999, pp. 52-59.
- [6] E. Gill, O. Montenbruck, J.M. Fraile-Ordonez, "Orbit Determination of the MIR Space Station Using MOMSNAV GPS Measurements", 11th *International Astrodynamics Symposium/20th International Symposium on Space Technology and Science*, Gifu, Japão, 1996, pp. 295-300.